
Princeton Plasma Physics Laboratory

PPPL-

PPPL-



Prepared for the U.S. Department of Energy under Contract DE-AC02-09CH11466.

Princeton Plasma Physics Laboratory

Report Disclaimers

Full Legal Disclaimer

This report was prepared as an account of work sponsored by an agency of the United States Government. Neither the United States Government nor any agency thereof, nor any of their employees, nor any of their contractors, subcontractors or their employees, makes any warranty, express or implied, or assumes any legal liability or responsibility for the accuracy, completeness, or any third party's use or the results of such use of any information, apparatus, product, or process disclosed, or represents that its use would not infringe privately owned rights. Reference herein to any specific commercial product, process, or service by trade name, trademark, manufacturer, or otherwise, does not necessarily constitute or imply its endorsement, recommendation, or favoring by the United States Government or any agency thereof or its contractors or subcontractors. The views and opinions of authors expressed herein do not necessarily state or reflect those of the United States Government or any agency thereof.

Trademark Disclaimer

Reference herein to any specific commercial product, process, or service by trade name, trademark, manufacturer, or otherwise, does not necessarily constitute or imply its endorsement, recommendation, or favoring by the United States Government or any agency thereof or its contractors or subcontractors.

PPPL Report Availability

Princeton Plasma Physics Laboratory:

<http://www.pppl.gov/techreports.cfm>

Office of Scientific and Technical Information (OSTI):

<http://www.osti.gov/bridge>

Related Links:

[U.S. Department of Energy](#)

[Office of Scientific and Technical Information](#)

[Fusion Links](#)

Phase-space dynamics of runaway electrons in tokamaks

Xiaoyin Guan, Hong Qin, and Nathaniel J. Fisch

Princeton Plasma Physics Laboratory,

Princeton University, Princeton, NJ 08543, USA

Abstract

The phase-space dynamics of runaway electrons is studied, including the influence of loop voltage, radiation damping, and collisions. A theoretical model and a numerical algorithm for the runaway dynamics in phase space are developed. Instead of standard integrators, such as the Runge-Kutta method, a variational symplectic integrator is applied to simulate the long-term dynamics of a runaway electron. The variational symplectic integrator is able to globally bound the numerical error for arbitrary number of time-steps, and thus accurately track the runaway trajectory in phase space. Simulation results show that the circulating orbits of runaway electrons drift outward toward the wall, which is consistent with experimental observations. The physics of the outward drift is analyzed. It is found that the outward drift is caused by the imbalance between the increase of mechanical angular momentum and the input of toroidal angular momentum due to the parallel acceleration. An analytical expression of the outward drift velocity is derived. The knowledge of trajectory of runaway electrons in configuration space sheds light on how the electrons hit the first wall, and thus provides clues for possible remedies.

PACS numbers: 52.20.Dq,52.30.Gz,52.65.Cc

I. INTRODUCTION

In tokamaks, relativistic runaway electrons are often observed during and after a plasma disruption or during a fast plasma shutdown [1–4]. The growth-rate of avalanche runaway electron induced by knock-on process, synchrotron radiation and magnetic fluctuations has been studied extensively [5–7]. Runaway electrons can hit and damage the first wall [8]. In a long-pulse discharge with non-zero loop voltage, runaway electrons can hit and damage the wall even without disruption or fast shutdown. Also, during start-up with non-ohmic current-drive, runaway electrons can be produced in the direction opposing the current, presenting similar issues [9]. Previous research had focused on the energy limit of runaway electrons under the influence of loop voltage, synchrotron radiation, bremsstrahlung drag forces, and collisions [10–13]. The evolution path of a runaway electron in momentum space due to these four physical effects has been studied in details [14, 15]. The effects of stochastic magnetic field on the transport and energy limit of runaway electrons have also been studied [16–20].

On the other hand, the orbits of runaway electrons in configuration space, even without magnetic fields fluctuation, have not been thoroughly studied. However, a comprehensive understanding of the configuration space trajectory of runaway electrons is important, because it tells us how the electrons hit the first wall, and thus provides clues for possible remedies. In addition, the termination of runaway electron orbits in configuration space can also modify the maximum energy, especially for those electrons originated from the edge region. Based on the experimental observations on the Tore Supra tokamak and relevant orbit calculation [21], it was suggested that runaway electrons can shift far away from magnetic surfaces within one transit period, and the orbit will open to intersect the conducting wall. An early study in a small tokamak indicated that there are possible trajectories of runaway electrons which shift tens of millimeters outward and expand radially in a single toroidal pass [22]. More comprehensive theoretical and numerical studies are needed to understand the physics of runaway electrons drifting away from magnetic surfaces.

In this paper, we study runaway electron orbits in the phase space under the influences of loop voltage, synchrotron radiation, bremsstrahlung radiation and collisions in system time-scale. The loop voltage is modeled as an inductive electric field. The radiation damping of synchrotron and bremsstrahlung radiation is modeled as an effective force acting on

electrons. Collisional effect is included using the Monte-Carlo methods. To numerically calculate the phase space trajectory of runaway electrons, we adopt a variational symplectic integrator [23–25] with good global conservative properties over long integration time. This is because we need to guarantee that the numerical error accumulated over this very long-time scale is less than the size of the physical effects. For standard numerical integrators, coherent error accumulation over many time-steps can be significantly larger than the collisional effects and the long-term runaway dynamics. Therefore, it is crucial that we use a variational symplectic integrator for the guiding center dynamics to carry out the numerical simulation of runaway electrons. Through simulation studies, we discover that the circulating orbits of runaway electrons drift outward toward the wall, which is consistent with experimental observations. The physics of this outward drift is analyzed. It is found that the outward drift is caused by the imbalance between the increase of mechanical angular momentum and the input of toroidal angular momentum due to the parallel acceleration. We derive an analytical expression of the outward drift velocity, which is able to explain the main feature of the simulation results.

The paper is organized as follows. The theoretical model of a runaway electron and the symplectic variational integrator with good global conservative properties over long integration time are developed in Sec. II. In Sec. III, numerical results are presented and the physics of the outward drift of the circulating orbit of a runaway electron is analyzed, along with an analytical derivation of the outward drift velocity. Conclusions and future work are discussed in Sec. IV.

II. THEORETICAL MODEL AND NUMERICAL ALGORITHM

The relativistic guiding center Lagrangian, in the absence of the effects of radiation and collisions, can be written as [26]

$$L = (e\mathbf{A}_0 + e\mathbf{A}_1 + p_{\parallel}\mathbf{b}) \cdot \dot{\mathbf{x}} - \gamma mc^2, \quad (1)$$

where e is the charge, \mathbf{A}_0 is the vector potential of the equilibrium magnetic field, p_{\parallel} is the momentum along magnetic fields, \mathbf{b} is unit vector along magnetic fields, $\gamma = \sqrt{1 + p_{\parallel}^2/m^2c^2 + 2\mu B/mc^2}$ is the relativistic factor, B is the magnetic fields, $\mu = p_{\perp}^2/2mB$

is the magnetic momentum, p_{\perp} is the momentum perpendicular to the magnetic fields, m is the rest mass of the electron, and c is the speed of light. Here, the electric field due to the loop voltage is included as an inductive field,

$$\mathbf{E}_1 = -\frac{\partial \mathbf{A}_1}{\partial t}. \quad (2)$$

We now include the effects of radiation and collisions. For the radiation, previous studies have shown [10, 14, 15] that the radiation can be treated as a drag force in the opposite direction of the velocity of the particle, which is equivalent to an effective inductive electric field,

$$\mathbf{E}_{eff} = -\frac{\partial \mathbf{A}_{eff}}{\partial t}. \quad (3)$$

The magnitude of \mathbf{E}_{eff} is determined by

$$eE_{eff} = F_S + F_B, \quad (4)$$

where F_S represents synchrotron radiation drag force, and F_B represents bremsstrahlung friction force. They can be expressed as [10, 14, 15]

$$F_S = \frac{2}{3} r_e m c^2 \left(\frac{\sqrt{\gamma^2 - 1}}{\gamma} \right)^3 \gamma^4 \left(\frac{1}{R_0^2} + \frac{\sin^4 \theta}{r_g^2} \right), \quad (5)$$

$$F_B = \frac{4}{137} n_e (Z_{eff} + 1) m c^2 \gamma r_e^2 \left(\ln 2\gamma - \frac{1}{3} \right), \quad (6)$$

where R_0 is the major radius, $\sin \theta = p_{\perp}/p$ is the pitch angle, $r_g = p_{\perp}/eB_0$ is the electron gyro-radius, $r_e = e^2/4\pi\epsilon_0 m c^2$ is the classical electron radius, n_e is the plasma density, and Z_{eff} is the effective ionic charge. Therefore, our relativistic Lagrangian for the guiding center dynamics of a runaway electron with loop voltage and radiation effects is

$$L = (e\mathbf{A}_0 + e\mathbf{A}_1 + e\mathbf{A}_{eff,\parallel} + p_{\parallel}\mathbf{b}) \cdot \dot{\mathbf{x}} - \gamma m c^2, \quad (7)$$

where the magnetic momentum and relativistic factor are

$$\mu = \frac{p_{\perp}^2}{2mB} + \frac{eA_{eff,\perp}p_{\perp}}{2mB}, \quad (8)$$

$$\gamma = \sqrt{1 + \frac{p_{\parallel}^2}{m^2 c^2} + \frac{2 \left(\mu - \frac{e A_{eff, \perp} p_{\perp}}{2 m B} \right) B}{m c^2}}. \quad (9)$$

The collisional effects for runaway electrons are modeled by the Monte-Carlo method, where each collision induces changes in momentum space according to [2, 4, 11]

$$\Delta p_{\parallel} = -\frac{n_e e^4 \ln \Lambda m}{4 \pi \varepsilon_0^2} \gamma (Z_{eff} + 1 + \gamma) \frac{p_{\parallel}}{p^3} \Delta t = f(p_{\parallel}, p_{\perp}^2) \Delta t, \quad (10)$$

$$\Delta p_{\perp}^2 = \frac{2 n_e e^4 \ln \Lambda m}{4 \pi \varepsilon_0^2} \frac{\gamma}{p^3} [p_{\parallel}^2 (Z_{eff} + 1) - \gamma p_{\perp}^2] \Delta t = g(p_{\parallel}, p_{\perp}^2) \Delta t. \quad (11)$$

Here, $\ln \Lambda$ is the Coulomb logarithm. Note that the momentum is dominant in parallel direction, and the collisional effect is mainly the averaged slowing-down and momentum flow from the parallel direction to the perpendicular direction due to pitch-angle scattering.

To numerically solve for the phase-space dynamics of a runaway electron, the numerical integrator we use must have good global conservative properties over long integration time for the following two reasons. First, the time-scale of evolution of the runaway electrons due to loop voltage and radiation drag is much longer than the circulating period, typically many thousands times of the circulating period. Standard numerical integrators, such as the fourth-order Runge-Kutta method, can't track the trajectory accurately for such a long time [23–25]. This is because these standard integrators only guarantee that the error is small in each time-step. However, the errors at different time-steps often accumulate coherently and result in a large error over a large number of time-steps. Secondly, the collisional effects are usually small in each circulating period. To accurately simulate the long-term dynamics of a runaway electron and the collisional effects, we need to guarantee that the numerical error accumulated over this very long-time scale is less than the size of the physical effects. For standard numerical integrators, coherent error accumulation [23–25] over many time-steps can be significantly larger than the collisional effects and the long-term runaway dynamics. Therefore, it is crucial that we use a variational symplectic integrator for the guiding center dynamics [23–25] to carry out the numerical simulation of runaway electrons.

For simplicity, we consider a 2D tokamak model with circular concentric flux surfaces. In this geometry, there are two useful coordinate systems, the cylindrical coordinate system (R, ξ, z) and the toroidal coordinate system $(r, \theta, \bar{\xi} = -\xi)$, which are illustrated in Fig. 1.

The magnetic field is chosen to be

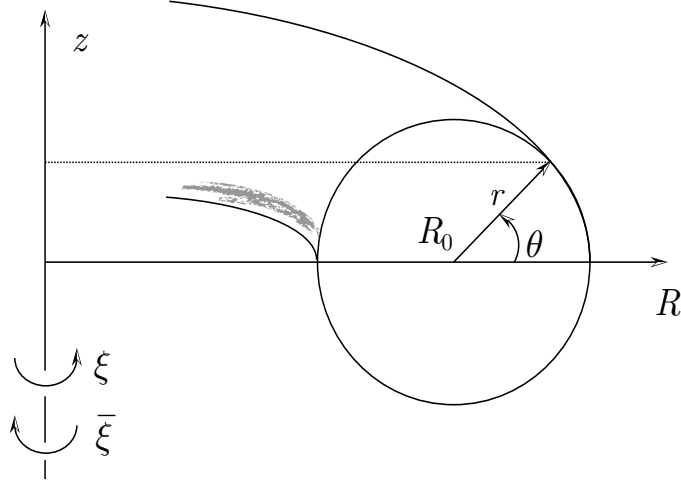


FIG. 1: 2D tokamak geometry with circular concentric flux surfaces.

$$\mathbf{B} = \frac{B_0 r}{qR} \mathbf{e}_\theta + \frac{B_0 R_0}{R} \mathbf{e}_\xi, \quad (12)$$

where B_0 , R_0 and q are constant with their usual meanings. The vector potential \mathbf{A}_0 , \mathbf{A}_1 , $\mathbf{A}_{eff,\parallel}$, $A_{eff,\perp}$, which correspond to the magnetic field, loop voltage, radiation drag force, are chosen to be

$$\mathbf{A}_0 = \frac{B_0 r^2}{2Rq} \mathbf{e}_\xi - \ln\left(\frac{R}{R_0}\right) \frac{R_0 B_0}{2} \mathbf{e}_z + \frac{B_0 R_0 z}{2R} \mathbf{e}_R, \quad (13)$$

$$\mathbf{A}_1 = E_1 t \frac{R_0}{R} \mathbf{e}_\xi, \quad (14)$$

$$\mathbf{A}_{eff,\parallel} = E_{eff,\parallel} t \mathbf{b}, \quad (15)$$

$$A_{eff,\perp} = E_{eff,\perp} t. \quad (16)$$

In this geometry, the relativistic guiding center Lagrangian is

$$L = (e\mathbf{A}_0 + e\mathbf{A}_1 + e\mathbf{A}_{eff,\parallel} + p_{\parallel} \mathbf{b}) \cdot \dot{\mathbf{x}} - \gamma m c^2 = p_r \dot{r} + p_\theta \dot{\theta} + p_\xi \dot{\xi} - H, \quad (17)$$

$$p_r = -e \ln\left(\frac{R}{R_0}\right) \frac{R_0 B_0}{2} \sin \theta + e \frac{R_0 B_0 z}{2R} \cos \theta, \quad (18)$$

$$p_\theta = -e \ln \left(\frac{R}{R_0} \right) \frac{R_0 B_0 r}{2} \cos \theta - e \frac{R_0 B_0 z}{2R} \sin \theta + \frac{(p_\parallel + eE_{eff,\parallel} t) r^2}{\sqrt{r^2 + R_0^2 q^2}}, \quad (19)$$

$$p_\xi = \left(e \frac{B_0 r^2}{2Rq} + \frac{(p_\parallel + eE_{eff,\parallel} t) R_0 q}{\sqrt{r^2 + R_0^2 q^2}} + eE_1 t \frac{R_0}{R} \right) R, \quad (20)$$

$$H = mc^2 \sqrt{1 + \frac{p_\parallel^2}{m^2 c^2} + \frac{2B}{mc^2} \left(\mu - \frac{eE_{eff,\perp} t p_\perp}{2mB} \right)}. \quad (21)$$

Because $\partial L / \partial \xi = 0$, we have

$$p_\xi = \frac{\partial L}{\partial \dot{\xi}} = \text{const.} \quad (22)$$

From Eq. (20), we can solve for p_\parallel in terms of the invariant p_ξ

$$p_\parallel = \left(p_\xi - e \frac{B_0 r^2}{2q} - \frac{eE_{eff,\parallel} t R_0 R q}{\sqrt{r^2 + R_0^2 q^2}} - eE_1 t R_0 \right) \frac{\sqrt{r^2 + R_0^2 q^2}}{R R_0 q}, \quad (23)$$

and substitute Eq. (23) into Eqs. (17)-(21). The 2D dynamics in the (r, θ) space is then determined by the Lagrangian

$$L = p_r \dot{r} + p_\theta \dot{\theta} - H, \quad (24)$$

which is obtained from Eq. (17) by removing the $p_\xi \dot{\xi}$ term. This is the Ruth reduction. The invariant p_ξ enters Eq. (24) parametrically.

To numerically solve for the runaway dynamics we apply the variational symplectic algorithm [23–25] to this 2D relativistic guiding center Lagrangian. In the simulation, we use coordinates (x, y) instead of (r, θ) . The first-order discretized Lagrangian corresponding to L in the time interval $t = [kh, (k+1)h]$ is [23–25]:

$$L_d(k, k+1) \equiv p_x(k, k+1) \frac{x_{k+1} - x_k}{h} + p_y(k, k+1) \frac{y_{k+1} - y_k}{h} - H(k, k+1). \quad (25)$$

The iteration relations for each step are

$$\frac{\partial}{\partial x_k} [L_d(k-1, k) + L_d(k, k+1)] = 0, \quad (26)$$

$$\frac{\partial}{\partial y_k} [L_d(k-1, k) + L_d(k, k+1)] = 0. \quad (27)$$

Collisional effects are included according to Eqs. (10) and (11),

$$\Delta p_{\parallel} = f(p_{\parallel}, p_{\perp}) \Delta t, \quad (28)$$

$$\Delta p_{\perp} = g(p_{\parallel}, p_{\perp}) \Delta t. \quad (29)$$

Equations (28) and (29) give us the iteration relations

$$\frac{(p_{\parallel}^{k+1} - p_{\parallel}^k)}{\Delta t} = f \left[\frac{p_{\parallel}^{k+1} + p_{\parallel}^k}{2}, \frac{p_{\perp}^{k+1} + p_{\perp}^k}{2} \right], \quad (30)$$

$$\frac{(p_{\perp}^{k+1} - p_{\perp}^k)}{\Delta t} = g \left[\frac{p_{\parallel}^{k+1} + p_{\parallel}^k}{2}, \frac{p_{\perp}^{k+1} + p_{\perp}^k}{2} \right], \quad (31)$$

where Δt is the time-step.

III. PHASE-SPACE DYNAMICS OF RUNAWAY ELECTRONS

Using the theoretical model and variational symplectic integrator developed in Sec. II, we now study the phase-space dynamic of a runaway electron in a typical tokamak. The major radius of the tokamak is taken to be $R_0 = 1m$, the on-axis magnetic field is $B_0 = 5T$, and the safety factor is $q = 2$. The loop voltage is chosen to be $5V/m$. The simulation time-step Δt in Eqs. (30) and (31) is chosen to be $5 \times 10^{-8}/\nu$, where $\nu = n_e e^4 \ln \Lambda / (4\pi \epsilon_0^2 m_e^2 c^3)$ is collision frequency for relativistic electrons. The simulation results of the phase space trajectory are displayed in Fig. 2. Plotted in Fig. 2(a) and Fig. 2(b) are runaway electron orbits in the configuration space projected onto a poloidal plane. Fig. 2(a) is result for an electron with collisions starting from the initial energy $E_0 = 3.35MeV$, initial momentum $p_{\parallel} = 5mc$ and $p_{\perp} = 1mc$, and initial position $x_0 = 0.1m$ and $y_0 = 0m$. The circulating orbits at different time are plotted. Fig. 2(b) is the same case as Fig. 2(a), but without collisions. Plotted in Fig. 2(c) and Fig. 2(d) are parallel momentum and square of perpendicular momentum of the same electron versus time. The black line is the collisional case, and the red line is the collisionless case. These results show clearly that the circulating orbit of runaway electron drifts outward toward the wall. By comparing the results with and without collisions, we observe that collisions have no significant effects on configuration space trajectory. But in

the momentum space, collisional effects are important. Perpendicular momentum increases significantly as a result of the pitch-angle scattering.

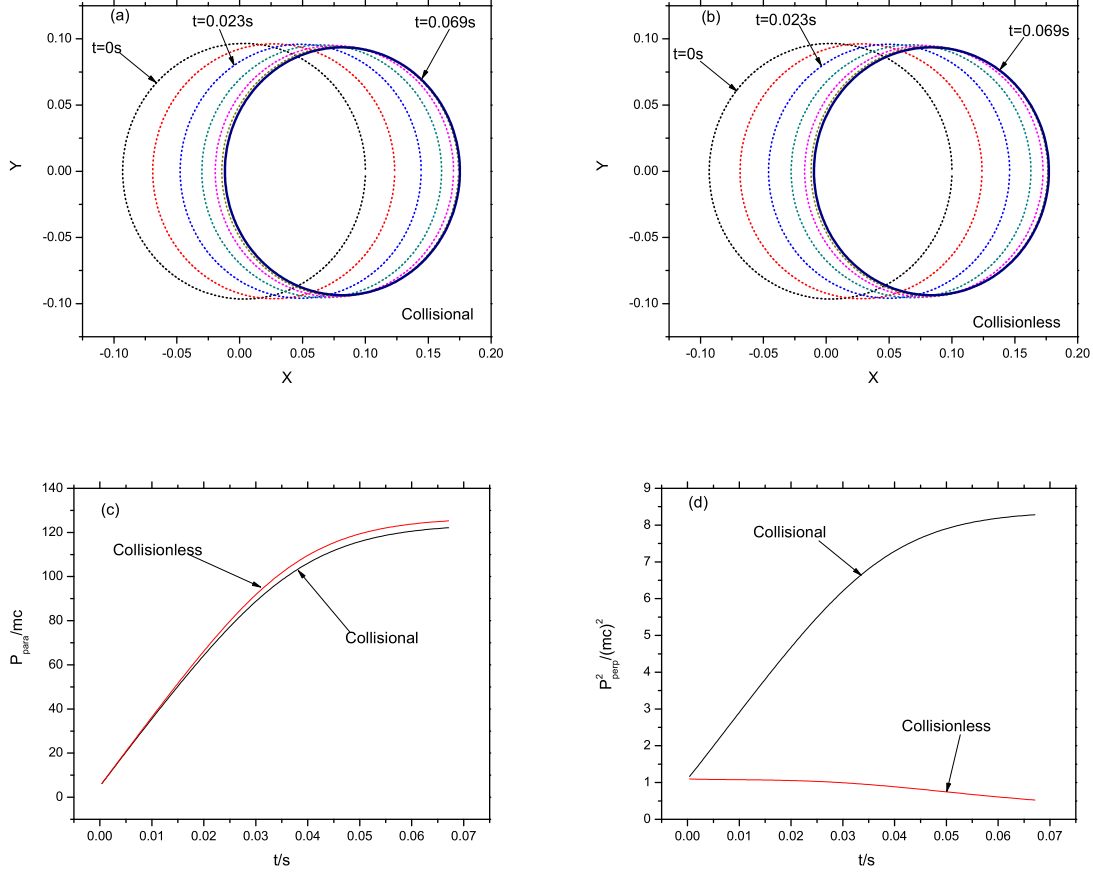


FIG. 2: (a) Runaway electron drift orbits with collisions starting from the initial energy $E_0 = 3.35MeV$, initial momentum $p_{\parallel} = 5mc$, $p_{\perp} = 1mc$ and initial position $x_0 = 0.1m$, $y_0 = 0m$. (b) The same case as (a), but without collisions. (c) Parallel momentum versus time for the same runaway electron with (black line) and without (red line) collisions. (d) Perpendicular momentum squared versus time for the same electron.

As mentioned in Sec.I, previous studies have been focused on the runaway dynamics in the momentum space [14, 15]. Here, we compare our simulation results with previous studies on momentum dynamics of runaway electrons [14, 15]. Fig.3(a) is the momentum trajectories of runaway electrons generated in our simulation. Different lines start from different initial conditions as marked in the figure. Fig.3(b) is the momentum trajectories of the same runaway electrons obtained using the numerical method reported in [14, 15].

Our results agree with previous results very well. There are some differences in the fine scale, which can be attributed to the fact that in our theoretical model, the momentum space and the configuration space are coupled, and in previous studies the momentum dynamics is decoupled from the configuration coordinates. The agreement displayed in Fig. 3 indicates that the previous assumption of momentum space being decoupled from the configuration space is indeed valid for the specific cases under investigation.

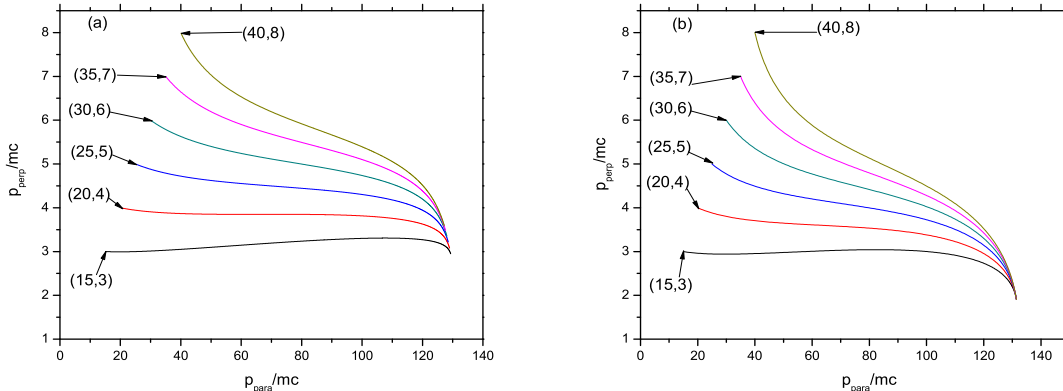


FIG. 3: (a) Momentum space trajectories for runaway electrons starting from initial momenta $(p_{\parallel}/mc, p_{\perp}/mc) = (15, 3), (20, 4), (25, 5), (30, 6), (35, 7), (40, 8)$. (b) Momentum space trajectories for the same runaway electrons using the method reported in [14, 15].

The outward drift of the circulating orbit of a runaway electron is mainly due to the parallel acceleration induced by loop voltage and radiation damping. We now analyze the physics of this outward drift, and develop an analytical model for it. Let's consider the guiding center orbit in a tokamak with the circular concentric flux. Assume that we select a fixed vertical position $y = r \sin \theta$. At the moment the guiding center of a runaway electron is crossing the height of y , we measure its horizontal position, toroidal angle, and parallel momentum to be (x, ξ, p_{\parallel}) . The guiding center comes back to the same height from the same side after one poloidal period Δt , and the phase space coordinates are shifted to $(x + \Delta x, \xi + \Delta \xi, p_{\parallel} + \Delta p_{\parallel})$. Our objective is to calculate Δx , and $\Delta x/\Delta t$ measures the outward drift velocity of the circulating orbit of the runaway electron. To calculate Δx , we use the conservation of toroidal angular momentum Eq. (22), and the energy equation

$$\Delta (\gamma mc^2) = \oint e (\mathbf{E}_1 + \mathbf{E}_{eff}) \cdot ds. \quad (32)$$

Equation (32) states that the increase of guiding center energy equals the work done by the loop voltage and radiation drag force. From Eq. (22) we have

$$\Delta p_\xi = 0. \quad (33)$$

The parallel momentum is always much larger than the perpendicular momentum, so for simplicity we only consider the radiation drag in the toroidal direction. Because the effects of the loop voltage and radiation drag in each poloidal period is small, we further assume that they can be treated as constants within each poloidal period. With these approximations, Eq. (32) and Eq. (33) can be expressed as

$$\Delta(\gamma mc^2) = \oint e(\mathbf{E}_1 + \mathbf{E}_{eff}) \cdot d\mathbf{s} \approx -e(E_1 + E_{eff,\parallel}) \oint R \dot{\xi} dt, \quad (34)$$

$$e \frac{B_0 x \Delta x}{q} + \Delta p_\parallel \frac{RR_0 q}{\sqrt{x^2 + y^2 + R_0^2 q^2}} + p_\parallel \Delta \left(\frac{RR_0 q}{\sqrt{x^2 + y^2 + R_0^2 q^2}} \right) + e(E_1 + E_{eff,\parallel}) R_0 \Delta t = 0. \quad (35)$$

The integration in Eq. (34) is the toroidal precession of the circulating guiding center [27]. It can be carried out along the unperturbed circulating orbit without outward drift. The quantities $\dot{\xi}$ and p_\parallel needed in the integration are obtained from the unperturbed relativistic guiding center Lagrangian L_0 without loop voltage and radiation drag force

$$L = (e\mathbf{A}_0 + p_\parallel \mathbf{b}) \cdot \dot{\mathbf{x}} - \gamma mc^2 = p_r \dot{r} + p_\theta \dot{\theta} + p_\xi \dot{\xi} - H, \quad (36)$$

$$p_r = -e \ln \left(\frac{R}{R_0} \right) \frac{R_0 B_0}{2} \sin \theta + e \frac{R_0 B_0 z}{2R} \cos \theta, \quad (37)$$

$$p_\theta = -e \ln \left(\frac{R}{R_0} \right) \frac{R_0 B_0 r}{2} \cos \theta - e \frac{R_0 B_0 z}{2R} \sin \theta + \frac{p_\parallel r^2}{\sqrt{r^2 + R_0^2 q^2}}, \quad (38)$$

$$p_\xi = \left(e \frac{B_0 r^2}{2Rq} + \frac{p_\parallel R_0 q}{\sqrt{r^2 + R_0^2 q^2}} \right) R, \quad (39)$$

$$H = mc^2 \sqrt{1 + \frac{p_\parallel^2}{m^2 c^2} + \frac{2\mu B}{mc^2}}. \quad (40)$$

The Euler-Lagrangian equations are

$$\frac{d}{dt} \frac{\partial L_0}{\partial \dot{x}_i} = \frac{\partial L_0}{\partial x_i}, (x_i = r, \theta, \xi, p_{\parallel}). \quad (41)$$

From Eqs. (36)-(41) we have

$$\dot{\xi} = \dot{\xi}^{(0)} + \dot{\xi}^{(1)} \cos \theta \varepsilon + O(\varepsilon^2), \quad (42)$$

$$\dot{p}_{\parallel} = \dot{p}_{\parallel}^{(1)} \sin \theta \varepsilon + O(\varepsilon^2), \quad (43)$$

where $\dot{\xi}^{(0)} = p_{\parallel}/R_0 m \sqrt{1 + p_{\parallel}^2/m^2 c^2 + 2\mu B_0/mc^2}$ and $\varepsilon = r/R_0$. From Eqs. (42) and (43), it's clear that to calculate the integration in Eq. (34) to $O(\varepsilon)$, we can use $R\dot{\xi} = R_0\dot{\xi}^{(0)}$, and $p_{\parallel} = \text{const}$. Therefore the toroidal precession is

$$\oint R\dot{\xi} dt \approx R_0\dot{\xi}^{(0)} \Delta t = \frac{p_{\parallel} \Delta t}{R_0 m \sqrt{1 + \frac{p_{\parallel}^2}{m^2 c^2} + \frac{2\mu B_0}{mc^2}}}. \quad (44)$$

Substituting Eq. (44) into Eq. (34) and keeping only the leading terms in terms of ε , we can solve for Δp_{\parallel} ,

$$\Delta p_{\parallel} = -e (E_1 + E_{eff,\parallel}) \Delta t + \frac{m\mu B_0 \Delta x}{p_{\parallel} R_0}. \quad (45)$$

Plugging Eq. (45) into Eq. (35) to eliminate Δp_{\parallel} and keeping the leading terms in terms of ε , we have

$$\frac{eB_0 x}{q} \Delta x - e (E_1 + E_{eff,\parallel}) x \Delta t = 0. \quad (46)$$

In above derivation, we assume ρ/r to be small, where ρ is the gyro-radius. This is true even for a highly relativistic electron. For example, for an electron with momentum $p_{\parallel} \sim p_{\perp} \sim 100mc$ and total energy $E \sim 70MeV$, its gyro-radius in a $5T$ magnetic field is only about $3cm$, which is smaller than the minor radius. Equation (46) states that the outward drift velocity of the circulating orbit of a runaway electron is

$$v_{dr} = \frac{\Delta x}{\Delta t} = \frac{q (E_1 + E_{eff,\parallel})}{B_0}, \quad (47)$$

which is in the x -direction. This agrees exactly with the numerical results shown in Fig. 2. From above analysis, we note that this outward drift is caused by the imbalance between the

increase of mechanical angular momentum and the input of angular momentum due to the toroidal acceleration. The conservation of canonical angular moment in the toroidal direction requires the radial position of the electron to change to compensate for the imbalance.

The trajectories of runaway electron on poloidal plane have been discussed with details in previous work [28]. The orbits are treated as closed orbits, which are described by the equation [28]

$$(R - R_0 - d_{net-drift})^2 + z^2 = const, \quad (48)$$

where, R is the horizontal position of runaway electrons, R_0 is the magnetic axis position, $d_{net-drift}$ is the net-drift, i.e., the distance between the drift orbit and the flux surface, and z is the vertical position of runaway electrons. The net drift is a constant. The typical value of the net drift is the safety factor q times the gyroradius. However, the discussion doesn't include the effects of toroidal electric fields, radiation and collisions. We have found that, under the influence of toroidal electric fields, radiation and collisions, the orbits of runaway electrons are not closed. They can't be described by the above equation. The orbits of runaway electron drift away from flux surfaces toward to the first wall. The net drift is not a constant. It increases as time before the force balance of toroidal electric fields, radiation and collisions is reached. Eventually, the net drift can be comparable to the minus radius. Generally speaking, the overall trajectories of runaway electrons on poloidal plane are determined by the physics of radiation, collisions balancing with toroidal electric fields. However, collisions are less important than radiation since runaway electrons are relativistic.

Equation (47) looks similar to the Ware pinch velocity [29],

$$v_{ware} = \frac{E_1}{B_\theta}. \quad (49)$$

However they are not the same. The Ware-pinch is the pinch due to the effect of the toroidal electrical field on trapped particles. Equation (47), on the other hand, describes the drift of circulating orbits induced by the effective toroidal electrical field. Previously, the effect of toroidal electrical field on circulating particles was thought to be the usual $\mathbf{E} \times \mathbf{B}$ drift [29], i.e.,

$$\mathbf{v}_{dr0} = \frac{\mathbf{E} \times \mathbf{B}}{B^2}. \quad (50)$$

In tokamaks, it can be written as

$$v_{dr0} = \frac{EB_\theta}{B_0^2}, \quad (51)$$

which is smaller than the Ware pinch velocity by $O(\varepsilon^2)$. However, our analysis leading up to Eq.(47) shows that the drift velocity of circulating orbits due to toroidal electric field is actually one order larger than the $\mathbf{E} \times \mathbf{B}$ drift. It is smaller than the Ware pinch velocity by $O(\varepsilon)$ instead of $O(\varepsilon^2)$. It's not small enough to be neglected in the study of relativistic runaway electrons dynamics in tokamaks. The outward drift of circulating orbits is smaller than the Ware pinch because it is impossible to accelerate a trapped electron in the toroidal direction. All of the input of toroidal angular momentum needs to be balanced by the change of radial position. For circulating electrons, most of the angular momentum input is balanced by the increasing of mechanical angular momentum, and the imbalance is $O(\varepsilon)$ smaller, which results in an outward drift smaller than the Ware pinch velocity by $O(\varepsilon)$ in amplitude.

The analytical result in Eq.(47) is compared with simulation results in Fig.4(a) and Fig.4(c). Plotted in Fig.4(a) is the theoretical and simulated outward drift distance versus time for the case of Fig.2(a). Plotted in Fig.4(c) is the theoretical and simulated drift distance versus time for the case of Fig.2(b). These comparisons show that the analytical model leading to Eq.(47) captures the basic feature of the outward drift of the runaway electron. The effective electric fields of the loop voltage and radiation drag for the same electron are plotted in Fig.4(b) and Fig.4(d) for the cases corresponding to Fig.4(a) and Fig.4(c), respectively. We observe that when the effective electric field of radiation damping is approaching to that of the loop voltage, the drift motion slows down. This is consistent with the analytical result of Eq.(47). Again, by comparing the results with and without collisions, we observe that collisions have no significant effects on the outward drift. This is consistent with the results in Fig.2.

Finally, we emphasize that it's easy to verify that the outward drift of runaway electrons is indeed important for future tokamaks operated in steady state. For non-relativistic particles, the gyrocenter orbit is typically close to a flux surface. The fact that circulating orbits of runaway electrons drift away from flux surfaces may raise the question whether this kind of orbit is consistent with the gyrocenter approximation. In order for the gyrocenter approximation to be correct, we only need the gyro-radius to be smaller than the scale-length

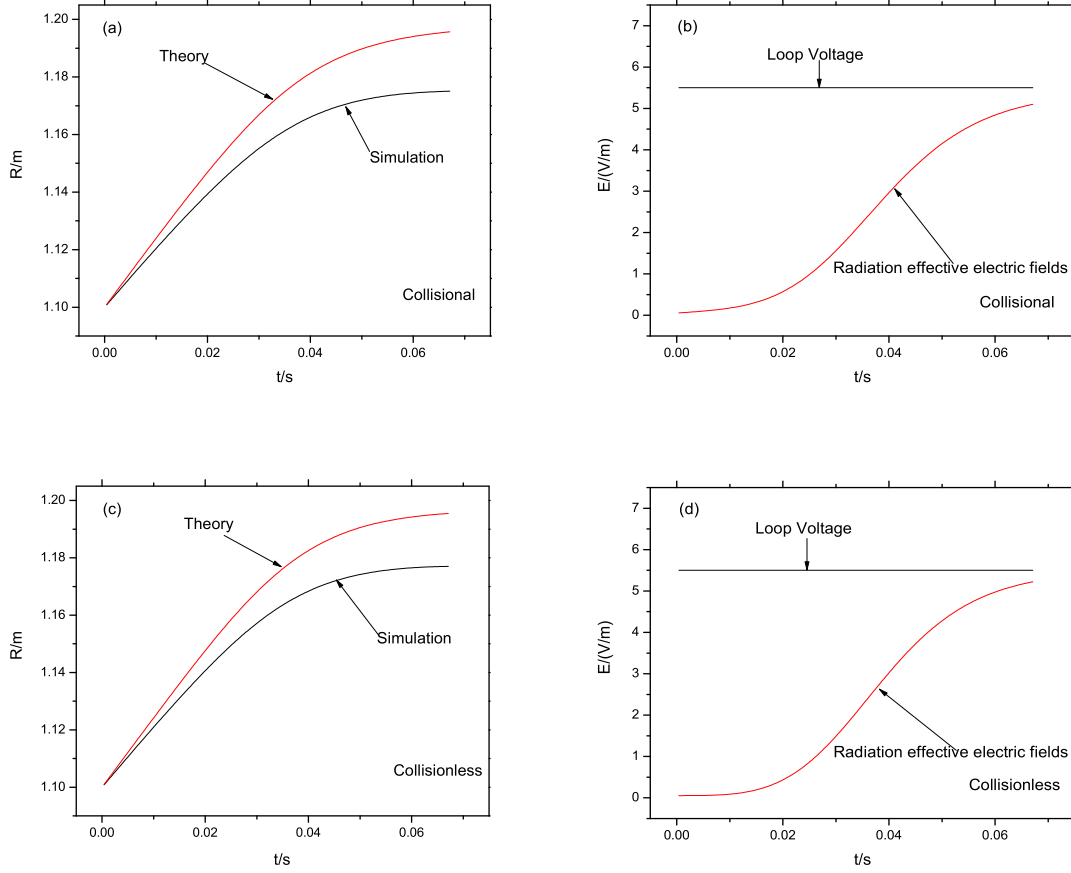


FIG. 4: (a) The theoretical and simulated drift motion for a runaway electron which starts from the initial energy $E_0 = 3.35\text{MeV}$, initial momentum $p_{\parallel} = 5mc$, $p_{\perp} = 1mc$ and initial position $x_0 = 0.1m$, $y_0 = 0m$ with collisions. (b) The effective electric field of the loop voltage and radiation for the same electron as in (a). (c) The theoretical and simulated drift motion for the same runaway electron without collisions. (d) The effective electric field of the loop voltage and radiation drag for the same runaway electron as in (c).

of the magnetic field. As calculated before, even for a 75MeV runaway electron with a large perpendicular momentum $p_{\parallel} \sim 140mc$ and $p_{\perp} \sim 40mc$ in a $2T$ magnetic field, the gyroradius is $3cm$. Therefore, for typical relativistic runaway electrons, the gyrocenter approximation is valid. To estimate the net departure of the orbit, we address the definition of the departure first. If the displacement is defined as the maximum displacement of a runaway electron relative to the closed flux surface that it starts from in one poloidal period, then it can be estimated as

$$d_1 \sim \frac{2q\pi p_{\parallel}}{eB_0}. \quad (52)$$

The following is a simple derivation of this estimate. In one poloidal period of the circulating orbit, the total distance that the electron travels along the field line is $2\pi R_0 q$. The time for this one poloidal period is therefore $2\pi R_0 q/v_{\parallel}$. Because the drift velocity relative to the closed flux surface is $v_d \sim p_{\parallel}^2/\gamma m_e e B R$, with assumption that the drift velocity is a constant, the maximum displacement relative to the closed flux surface in one poloidal period can be estimated as $d_1 \sim (2\pi R_0 q/v_{\parallel})(p_{\parallel}^2/\gamma m_e e B R) \sim \frac{2q\pi p_{\parallel}}{eB_0}$. If the displacement is defined as the distance between the center of the runaway orbit and the magnetic axis, then it is estimated to be [28]

$$d_2 \sim \frac{qP_{\parallel}}{eB_0}. \quad (53)$$

This estimate is a result of toroidal angular momentum conservation. The difference between the above two estimations is caused by how the displacement is defined. There is no real difference in terms of physics. However, we believe that Eq.(53) should be used when assessing whether or not the runaway electron reaches the wall, because Eq.(53) measures the net displacement of runaway electron away from magnetic axis. Now we will use Eq.(53) to estimate how large this displacement can be. Considering a tokamak machine which can maintain a steady state for 10sec with magnetic field $B \sim 2T$, safety factor $q \sim 2$, $Z_{eff} \sim 2$ and loop voltage $V \sim 0.1V$, a runaway electron in this tokamak can easily gain an energy above $75MeV$ in $2 \sim 3sec$ which corresponding to $p_{\parallel} \sim 150m_e c$. The total displacement is $d_2 \sim 26cm$. The minor radii of Alcator C-Mod, EAST and DIII-D are about $21cm$, $45cm$ and $50cm$, respectively. The toroidal magnetic fields of these three tokamaks are about $5T$, $2T$ and $2T$ [30–32]. The estimation of $d_2 \sim 26cm$ is comparable to any minor radii listed above. Therefore, the drift motion of runaway electron under influence of toroidal electric field is indeed important.

In addition, even for a large tokamak like ITER, the displacement of $d_2 \sim 26cm$ can result in important effects. For a tokamak operated in steady state, high power RF waves will be injected into the tokamak to maintain a preferred current profile. RF waves can pump electrons from lower energy region to higher energy region in which runaway electrons can be generated easily. Therefore a large amount of runaway electrons can be born at the location where RF wave power is absorbed, for example some location off-center. For these runaway electrons born at off-center location, the displacement $d_2 \sim 26cm$ is large enough for them to hit the first wall.

IV. DISCUSSION AND CONCLUSIONS

The phase-space dynamics of runaway electrons in tokamaks has been studied in this paper. We developed a physical model for runaway electrons under the influence of the loop voltage, radiation drag and collisions. In this model, we treat the loop voltage and radiation drag as inductive electric fields. The collisions are modeled by the Monte-Carlo method. To numerically simulate the long-term dynamics of a runaway electron, we applied a variational symplectic algorithm for the guiding center of electrons. The variational symplectic algorithm adopted has good global conservative properties over long integration times and thus is more suitable for simulating the runaway dynamics, compared with standard integrators which often have coherent error accumulation over a large number of time-steps. The physics of this outward drift is analyzed. It is found that the outward drift is caused by the imbalance between the increase of mechanical angular momentum and the input of toroidal angular momentum due to the parallel acceleration. An analytical expression of the outward drift velocity is derived. The knowledge of trajectory of runaway electrons in configuration space sheds light on how the electrons hit the first wall, and thus provides clues for possible remedies.

Note that, in this paper, we considered only the phase-space dynamics of an electron after it becomes a runaway electron, or, in other words, we considered only those electrons whose initial coordinates in phase space are such that the probability of it running away (that is to reach unbounded energy) is essentially unity. More generally, we could have considered with the same formalism those electrons whose probability of running away is not necessarily unity, that is, that there is a finite chance that the electron might reach zero velocity due to collisional effects before it reaches unbounded energy [33]. Such electrons are particularly important to consider in the case of rf heating or current drive, where the presence of the rf waves can produce runaway electrons by accelerating particles to regions in phase space of higher runaway probability.

In addition, we further restricted our present attention to electrons whose runaway dynamics is immediate or *prompt*, rather than after spending some time as thermal electrons. Thus we excluded the so-called *backward runaways*, which are produced during non-inductive start-up but change direction before running away. We also excluded those electrons that are initially trapped, and then only after several bounce periods become runaways. Note that

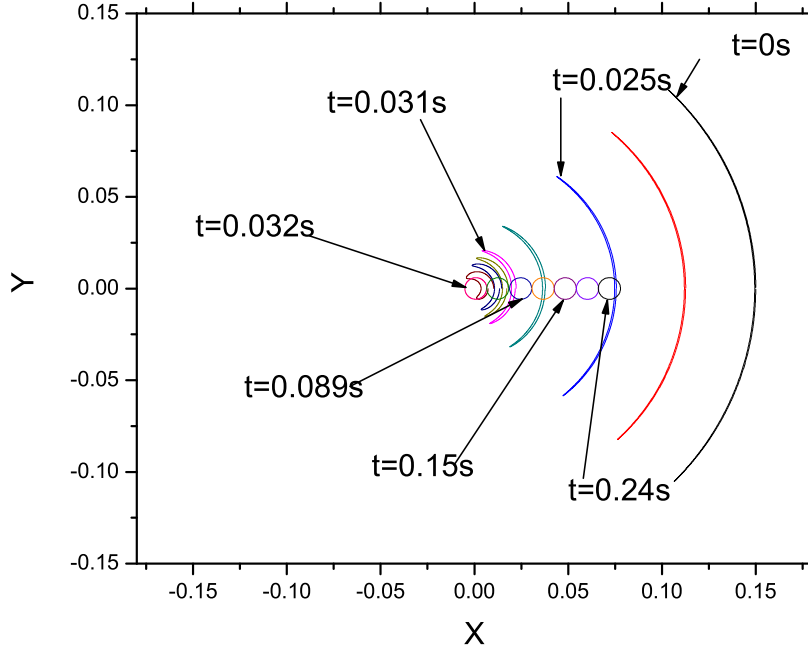


FIG. 5: Path in the configuration space of an initially trapped thermal electron being accelerated to become a runaway electron under a loop voltage of $5V$ olts.

the physical process associated with such electrons can be both complex and interesting. For example, the simulation result plotted in Fig. 5 shows how a trapped thermal electron with an initial energy $17KeV$ first undergoes the Ware pinch under a loop voltage of $5V$ olts, and then it is untrapped at a smaller radius. It subsequently becomes a runaway electron under the effect of the same loop voltage, and the circulating orbit moves outward toward the wall. The energy of the electron reaches $52MeV$ at $t = 0.24$ S. Such electrons, and for that matter the backward runaway electrons well, may strike the tokamak limiter at a different time and at a different location than would the runaway electrons that we considered, thus leaving a unique signature. The exploration of the paths in the configuration space of the electrons that are not prompt runaways is, however, left to a future study, where it is anticipated that the symplectic algorithms developed here will be usefully applicable.

Acknowledgments

This research was supported by the U.S. Department of Energy under contract No. DEAC02-76-CH03073.

- [1] H. Dreicer, *Physical Review Letters* **115**, 238 (1959).
- [2] R. M. Kulsrud, Y. C. Sun, N. K. Winsor, and H. A. Fallon, *Physical Review Letters* **31**, 690 (1973).
- [3] M. Murakami, S. C. Aceto, E. Anabitarte et al. *Physics of Fluids B* **3**, 2261 (1991).
- [4] M. N. Rosenbluth and S. V. Putvinski, *Nuclear Fusion* **37**, 1355 (1997).
- [5] J. R. Martin-Solis, R. Sanchez, and B. Esposito, *Physics of Plasmas* **7**, 3369 (2000).
- [6] P. B. Parks, M. N. Rosenbluth, and S. V. Putvinski, *Physics of Plasmas* **6**, 2523 (1999).
- [7] S. C. Chiu, M. N. Rosenbluth, R. W. Harvey, and V. S. Chan, *Nuclear Fusion* **38**, 1711 (1998).
- [8] S. V. Putvinski, P. Barabaschi, N. Fujisawa, N. Putvinskaya, M. N. Rosenbluth, and J. Wesley, *Plasma Physics and Controlled Fusion* **39**, B157 (1997).
- [9] N. J. Fisch, *Reviews of Modern Physics* **59**, 175 (1987).
- [10] J. R. Martin-Solis, B. Esposito, R. Sanchez, and J. D. Alvarez, *Physics of Plasmas* **6**, 238 (1999).
- [11] B. Esposito, J. R. Martin-Solis, F. M. Poli, J. A. Mier, R. Sanchez, and L. Panaccione, *Physics of Plasmas* **10**, 2350 (2003).
- [12] F. Andersson, P. Helander, and L. G. Eriksson, *Physics of Plasmas* **8**, 5221 (2001).
- [13] M. Bakhtiari, G. J. Kramer, M. Takechi, H. Tamai, Y. Miura, Y. Kusama, and Y. Kamada, *Physical Review Letters* **94**, 215003 (2005).
- [14] J. R. Martin-Solis, J. D. Alvarez, R. Sanchez, and B. Esposito, *Physics of Plasmas* **5**, 2370 (1998).
- [15] M. Bakhtiari, G. J. Kramer, and D. G. Whyte, *Physics of Plasmas* **12**, 102503 (2005).
- [16] A. B. Rechester and M. N. Rosenbluth, *Physical Review Letters* **40**, 38 (1978).
- [17] L. Laurent and J. M. Rax, *Europhysics Letters* **11**, 219 (1990).
- [18] J. R. Myra and J. Catto, *Physics of Fluids B* **4**, 176 (1992).
- [19] B. Kurzan, K. H. Steuer, and G. Fussmann, *Physical Review Letters* **75**, 4626 (1995).

- [20] J. R. Martin-Solis and R. Sanchez, *Physics of Plasmas* **15**, 112505 (2008).
- [21] R. Nygren, T. Lutz, D. Walsh, G. Martin, M. Chatelier, T. Loarer, and D. Guilhem, *Journal of Nuclear Materials* **241**, 522 (1997).
- [22] E. Nishimura, *Japanese Journal of Applied Physics* **22**, 7 (1983).
- [23] H. Qin and X. Guan, *Physical Review Letters* **100**, 035006 (2008).
- [24] H. Qin and X. Guan, *Physics of Plasmas* **16**, 042510 (2009).
- [25] J. E. Marsden and M. West, *Acta Numerica* **10**, 357 (2001).
- [26] C. Grebogi and R. G. Littlejohn, *Physics of Fluids* **27**, 8 (1984).
- [27] Ya. I. Kolesnichenko, R. B. White, and Yu. V. Yakovenko, *Physics of Plasmas* **10**, 1449 (2003).
- [28] H. Knoepfel and D. A. Spong, *Nuclear Fusion* **19**, 785 (1979).
- [29] A. A. Ware, *Physical Review Letters* **25**, 15 (1970).
- [30] E. S. MarMar, et al. *Fusion Sci. Technol* **51**, 261-265 (2007).
- [31] Y. Shi, et al. *Review of scientific instruments* **81**, 033506 (2006).
- [32] G. L. Jackson, et al. *Nucl. Fusion* **48**, 125002 (2008).
- [33] C. F. F. Karney and N. J. Fisch, *Physics of Fluids* **29**, 180 (1986).

The Princeton Plasma Physics Laboratory is operated
by Princeton University under contract
with the U.S. Department of Energy.

Information Services
Princeton Plasma Physics Laboratory
P.O. Box 451
Princeton, NJ 08543

Phone: 609-243-2750
Fax: 609-243-2751
e-mail: pppl_info@pppl.gov
Internet Address: <http://www.pppl.gov>